Ocean Engineering 62 (2013) 10–24

Contents lists available at SciVerse ScienceDirect

Ocean Engineering

journal homepage: www.elsevier.com/locate/oceaneng

Experimental study on vortex-induced motions of a semi-submersible platform with four square columns, Part II: Effects of surface waves, external damping and draft condition

Rodolfo T. Gonçalves [a,*], Guilherme F. Rosetti [a], André L.C. Fujarra [a], Allan C. Oliveira [b]

[a] TPN—Numerical Offshore Tank, Department of Naval Architecture and Ocean Engineering, Escola Politécnica—University of São Paulo, Av. Professor Mello Moraes, 2231, Cidade Universitária, São Paulo, SP 05508-030, Brazil
[b] CENPES—Research and Development Center, Petrobras, Rio de Janeiro, RJ, Brazil

ARTICLE INFO

Article history:
Received 3 July 2012
Accepted 7 January 2013
Available online 17 February 2013

Keywords:
Vortex-induced motions (VIM)
Semi-submersible
Model tests
6 degrees-of-freedom (6 DOF)
Wave incidence
Damping level
Draft condition

ABSTRACT

Aiming to complete the results presented before by Gonçalves et al. (2012d. Ocean Eng. 54, 150–169) the present work brings new experimental results on VIM of a semi-submersible platform with four square columns, particularly concerning changes in three different aspects: simultaneous presence of current and surface waves in the same direction, external damping level, and draft conditions. The VIM tests were performed in the presence of regular and irregular waves, both conditions with simultaneous current presence, to understand the wave effects. Considerable differences between the presences of regular and irregular waves were observed. The motion amplitudes in the transverse direction, in the tests with regular waves, were markedly lower than those with irregular waves, and the VIM behavior was not observed. In the sea state tests, the amplitudes are lower than current-only ones, yet a periodic motion characterized by VIM was observed. Furthermore, the effects of the lower draft condition and damping level were addressed, showing they are important for model tests because they contribute to decreasing VIM amplitudes.

1. Introduction

As opposed to what happens with cylindrical platforms such as monocolumns and spars, the study on vortex-induced motions (VIM) phenomenon of semi-submersibles is quite more recent and, therefore, much less can be found about it, which probably happens because this phenomenon was only noticed after the increase in size of the new semi-submersibles, mainly the dimension of their columns. Nevertheless, important works can be cited, among which Rijken et al. (2004, 2011), Waals et al. (2007), Rijken and Leverette (2008), Hong et al. (2008), Hussain et al. (2009), Magee et al. (2011), Tahar and Finn (2011), Martin and Rijken (2012) and Xu et al. (2012). In a previous work, Gonçalves et al. (2012d) performed a series of tests to verify the influence of the incidence angle of current and the hull appendages on VIM of a semi-submersible with four square columns. The main results showed that VIM in the transverse direction occurred in a range of $4.0 \leq V_r \leq 14.0$ with amplitude peaks around $7.0 \leq V_r \leq 8.0$. The largest amplitudes obtained were around 40% of the column width for 30 and 45-degree incidences. Another important result observed was a considerable yaw motion oscillation, also denominated vortex-induced yaw (VIY), in which a synchronization region could be identified as a resonance phenomenon. The largest yaw motions were verified for the 0 and 180-degree incidences and the maxima angular amplitudes around 4.5 °.

There are a number of other aspects that are relevant on VIM of floating platforms, as discussed in Gonçalves et al. (2012c) and Fujarra et al. (2012), and the following can be mentioned: current incidence angle; hull appendages; simultaneous presence of surface waves and current incidence; draft conditions and external damping caused, for instance, by risers and mooring lines.

Under this context and aiming to complete the results presented before, the present work brings new experimental results on VIM of the same semi-submersible platform, illustrated in Fig. 1, concerning the three important remaining aspects: simultaneous presence of current and surface waves in the same direction, external damping level, and draft conditions.

Section 2 presents a background of the effects of surface waves, damping level and draft condition on the VIM phenomenon, as well as a background of fundamental studies in the same

* Corresponding author. Tel./fax: +55 11 30911727.
E-mail addresses: rodolfo_tg@tpn.usp.br (R.T. Gonçalves), guilherme.feitosa@tpn.usp.br (G.F. Rosetti), afujarra@usp.br (A.L.C. Fujarra), allan_carre@petrobras.com.br (A.C. Oliveira).

0029-8018/$ - see front matter © 2013 Elsevier Ltd. All rights reserved.
http://dx.doi.org/10.1016/j.oceaneng.2013.01.019

Nomenclature

ω	Instantaneous frequency
α	Velocity ratio
σ_u	RMS value of the fluid velocity of oscillatory flow
Φ	Incidence angle of current
ζ_L	Nondimensional linear damping coefficient
A	Characteristic yaw motion amplitude
A_p	Submerged projected area
A_x/L	Nondimensional characteristic motion amplitude in the in-line direction
A_y/L	Nondimensional characteristic motion amplitude in the transverse direction
b	Linear damping coefficient from the linear motion equation
b_1	Linear damping coefficient from the non-linear motion equation
b_2	Quadratic damping coefficient from the non-linear motion equation
C_a	Added mass coefficient
C_D	Drag force coefficient
C_L	Lift force coefficient
D	Characteristic dimension of the section of the body subjected to a vortex shedding
f_N	Natural frequency in still water
f_p	Peak frequency
f_{Rw}	Regular oscillatory flow frequency
f_{RW}	Regular wave height
H	Immersed column height above the pontoon
H_{RW}	Regular wave height
H_s	Significant wave height
$H(\omega,t)$	Hilbert spectrum
k	Stiffness coefficient
KA	Wave steepness
KC	Keulegan–Carpenter number
KC_r	Equivalent KC for irregular oscillatory flow
L	Column width
m	Structural mass of the platform
m_a	Added mass in the transverse direction
P	Pontoon height
Re	Reynolds number
S	Distance between center columns
St	Strouhal number
t	Time
T_N	Natural period in still water
T_o	Natural period of motion in the transverse direction in still water
T_p	Peak period
U	Incident current velocity
U_M	Maximum flow velocity
U_w	Oscillatory flow velocity
V_r	Reduced velocity
X	Axis motion in the in-line direction to the flow
Y	Axis motion in the transverse direction to the flow

subjects. The experimental setup and details about the reduced scale model are described in Section 3. The results and comparison concerning characteristic motion amplitudes for motions in the transverse and in-line directions, as well as characteristic yaw motion amplitudes are discussed in Section 4. Finally, in Section 5, the conclusions are drawn.

2. Background

2.1. Effect of surface wave on VIM of offshore floating units

The problem of wave and current induced motions of floating production systems was first studied without the vortex shedding effects; Tung and Huang (1973), Sarpkaya and Isaacson (1981) and Faltinsen (1994) can be cited as examples. Considering the vortex shedding effects, the research can be divided into three groups: effect of waves, of current and of simultaneous waves and current.

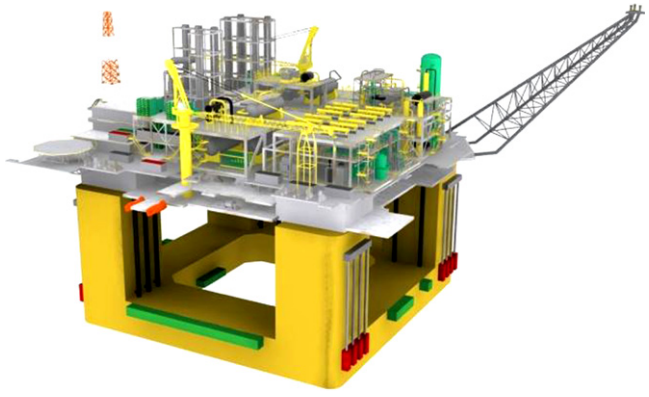

Fig. 1. Illustration of a semi-submersible with four square columns.

As one example, Borthwick and Herbert (1988) studied loading and responses of a cylinder in waves and showed that measured in-line forces and displacements generally had a dominant component in the wave frequency, but secondary peaks corresponding to the vortex shedding phenomenon and its harmonics were noticeable on the force and displacement traces. The transverse forces and displacements were considerable when the frequency of wave, f_{RW}, and transverse natural frequency, f_n, are similar, i.e., at the resonant region they are amplified. The results also depend on Keulegan–Carpenter numbers, KC; this nondimensional parameter will be discussed further on.

Another way to study the effect of oscillating flow on vortex shedding is to impose oscillatory motions in the in-line direction of an elastically mounted cylinder free to vibrate transversely, as for example the one studied by Sumer and FredsØe (1988), for regular oscillatory flow; and also by Kozakiewicz et al. (1994), for irregular condition. The transverse response depends on the ratio of frequencies of the oscillatory flow and the natural frequency of the system, f_{RW}/f_N; Keulegan–Carpenter number, KC; reduced velocity, V_r; and also on the Reynolds number.

As described in Sumer and FredsØe (1988), under regular (sinusoidal) oscillatory flow, the KC is defined by

$$KC = \frac{U_M}{f_{RW}D} \tag{1}$$

where U_M is the maximum flow velocity defined by:

$$U_w(t) = U_M \sin(2\pi f_{RW} t) \tag{2}$$

On the other hand, as described in Kozakiewicz et al. (1994), under irregular oscillatory flow, the equivalent KC_r are defined by

$$KC_r = \frac{\sqrt{2}\sigma_U}{f_p D} \tag{3}$$

where σ_U is the RMS value of the fluid velocity of oscillatory flow and f_p is the peak frequency of the flow.

A quasi wave-current co-existing field can be easily obtained either by oscillating a cylinder in the in-line direction in a uniform flow, as in Moreau and Huang (2010), or by moving it at a constant speed in a harmonically oscillating flow, as presented in Iwagaki and Asano (1984). Both methods showed that another important parameter beyond *KC* is the ratio α defined as:

$$\alpha = \frac{\sigma_U}{\sigma_U + U} \tag{4}$$

where U is the mean current velocity. This ratio becomes 1 at the limit of wave-only and tends to 0 as the current becomes large as compared with the oscillatory component. According to Iwagaki and Asano (1984), the plot of α vs. *KC* showed the ratio of viscous force to the inertia force. This result will be very important to understand the phenomenon of vortex-shedding and oscillatory flow, as will be discussed further on.

The study of the effects of surface wave on VIM of offshore floating units is more recent. In practice, DNV (2007, 2008) the effects of waves and current on VIM are discussed. The following statement can be extracted from DNV (2008): *"VIM analysis concentrates on the effect of current. The frequencies of incoming waves are unlikely to cause vortex shedding loads in the vicinity of the low natural frequencies for sway and roll. If wind and waves are present at the same time as currents causing VIM, then they will certainly affect the system response. It seems plausible that the wave-induced fluid velocities will tend to disorganize the combined velocity field, as compared to a pure current field, and be more likely to reduce the mean amplitude of the lift force due to vortex shedding, than to increase it. Hence, it should be conservative to superimpose the forces calculated separately due to waves and vortex shedding"*. It may be noted that it is not easy to quantify those phenomena together. Another difficulty is the small number of references available about this subject in the open literature. Among the works discussing VIM together with wave effects, Van Dijk et al. (2003), Irani and Finn (2005) and Finnigan et al. (2005) on spar platforms; Cueva et al. (2006), Gonçalves et al. (2010b) and Saito et al. (2012) on monocolumn platforms; and more recently, Rijken and Leverette (2008), Hong et al. (2008) and Martin and Rijken (2012) on semi-submersibles can be cited.

Finnigan et al. (2005) compared motions in the transverse direction due to current only and due to current with simultaneous wave presence on a spar platform. The waves were simulated as sea conditions with different wave heights. The results showed decreasing motions in the transverse direction for higher waves in the same direction of the current. A similar behavior was reported in Gonçalves et al. (2010b) for a monocolumn platform, but with regular waves and current in the same direction. These authors conjectured that the platform motions due to waves were capable of disturbing the vortex shedding resulting low VIM responses; and if the platform motions due to waves were small, then the VIM with and without waves were similar.

On the other hand, Rijken and Leverette (2008) performed VIM tests of semi-submersible platforms with waves aligned to the current as a sea condition and concluded that the presence of waves time delayed the onset of VIM; however, similar magnitude oscillations were observed. In the same way, Hong et al. (2008) carried out VIM tests with waves aligned to the current as a sea condition, and they concluded that the wave-induced particle velocity disturbs the VIM. Even so, few conditions were tested to answer the questions about wave effects. More recently, Martin and Rijken (2012) investigated the effect of operational sea states on VIM; the authors showed that the operational sea state had minimal effect on the VIM response of a semi-submersible.

Two works presented VIM results for wave transverse to the current direction. For a spar platform, Finnigan et al. (2005) showed that the transverse motions can be larger than the response in the current alone, but this statement depends on the heading. In the same way, Saito et al. (2012) performed tests for a monocolumn platform, showing similar results.

Therefore, in this work VIM model tests were performed in the presence of three regular waves and also three different conditions of sea state, all of them aligned to the current.

2.2. Effect of damping levels on VIM of offshore floating units

The simultaneous presence of risers and mooring lines is surely another aspect which interferes with the VIM response, i.e., external damping levels. It is therefore a subject that deserves further investigation, particularly under two points of view. The first concerns the change in the shedding pattern near the platform, hence the change of the hydrodynamic forces. The second refers to the drag increase, which has an important effect on the damping imposed on the floating unit.

van Dijk et al. (2003) attested the difficulty in simulating the presence of risers in VIM model tests of spar platforms, but the need to establish a procedure to include this effect is clear. Gonçalves et al. (2010b) carried out VIM tests using a device to represent, in scale, the damping due to the mooring lines and risers on monocolumn platforms. The results showed a decreasing on the VIM responses with the increase of external damping.

According to Rijken and Leverette (2008), the response amplitudes on a deep-draft semi-submersible were not significantly affected for equivalent linear damping up to 10% but showed a delay of VIM to higher reduced velocities. Complementarily to this work, Martin and Rijken (2012) increased the damping level at horizontal plane up to 17%, and under certain conditions the VIM response was reduced, suggesting a cause for the lower field-observed VIM responses.

Fundamental research of the effect of damping on amplitude and frequency on VIV of circular cylinders were performed recently by Jauvtis and Williamson (2004), Klamo et al. (2006) and Blevins and Coughran (2009). All the works showed the importance of the mass-damping parameter, i.e., the mass ratio multiplied by the structural damping level. Lower mass damping system presents higher amplitude levels, as well as the results for floating units cited above.

2.3. Effect of draft condition on VIM of offshore floating units

Looking for fundamental investigations into the influence of the cylinder length on the VIV phenomenon, it was possible to verify that most of the available studies are related to fixed cylinders under the effects of a free end. The free end effects influence on 1 degree-of-freedom (DOF) cylinder was reported in Morse et al. (2008); in this work, the results showed the absence of lower branch when the free end is exposed to the flow. Someya et al. (2010) performed 2 DOF tests with low aspect ratio cylinder in a limited range of reduced velocities $V_r \leq 4.50$. The works by Gonçalves et al. (2010a, 2012b) presented a series of tests with 2 DOF cylinders with low aspect ratio and compared the results with high aspect ratio cylinders. The maximum amplitudes are similar for a range $1.50 \leq L/D \leq 2.00$ compared with high aspect ratio $L/D \geq 6.00$, but decreasing with lower aspect ratio. Again, the absence of lower branch was verified; another important result was the changes in Strouhal number, the St decreases with lower aspect ratios as in fixed cylinder results, e.g., Fox and Apelt (1993).

The aspect ratio is then an important issue to be considered in the initial design phase of offshore platforms; the columns or the region of circular structures exposed to the flow can be adjusted to be less influenced by the vortex-shedding and, consequently, by lift forces.

In an offshore scenario, Gonçalves et al. (2010b) performed VIM tests on a monocolumn platform and showed that this aspect decreased the VIM response, mainly the lower draft conditions. Even for semi-submersibles, these aspects showed to be important. Waals et al. (2007) and Magee et al. (2011) pointed out lower amplitudes for lower draft conditions. Another way to change the aspect ratio of semi-submersible columns is improving their blister, as proposed in Xu (2011) and Xu et al. (2012); this feature also serves the purpose of breaking the vortex shedding coherence along the length of the column, decreasing the VIM amplitudes.

3. Experimental setup

The experimental setup is characterized by a small-scale model of the semi-submersible unit supported by a set of equivalent horizontal moorings in the towing tank at the Institute of Technological Research (IPT) in São Paulo, Brazil. The adopted scale was 1:100. More details about the reduced model can be found in the previous work by Gonçalves et al. (2012d). Table 1 and Fig. 2 present details of the semi-submersible small-scale model.

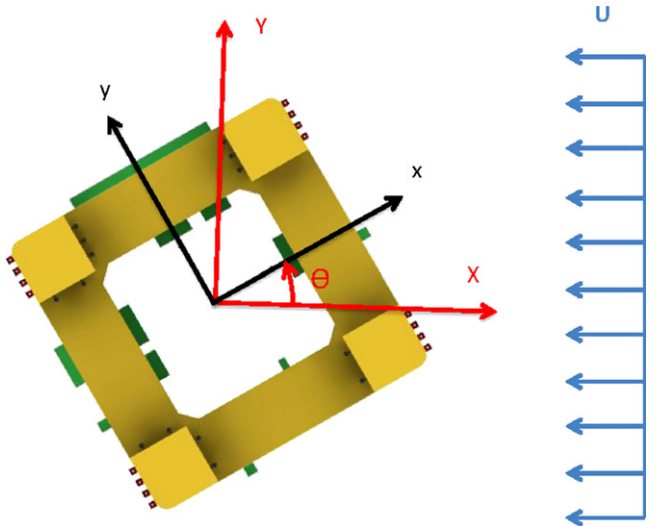

Fig. 3. Top view of the semi-submersible model showing the definition of incidence angles and hull appendages position.

Table 1
Main characteristics of the semi-submersible unit. Values in full scale.

Distance between center columns (S)	74.52 m
Column width (L)	19.80 m
Pontoon height (P)	11.40 m
Full draft ($H+P$)	34.00 m
Low draft ($H+P$)	16.00 m
Full displacement	105,237 t
Full inertial moment yaw	215×10^6 ton m^2
Low displacement	76,590 t
Low inertial moment yaw	159×10^6 t m^2

Table 2
JONSWAP sea condition characteristics without current incidence.

ID	Model scale–1:100		Full scale–1:1		KA
	f_p [Hz]	H_s [mm]	T_p [s]	H_s [m]	
1	0.67	65.23	14.93	6.52	5.9%
2	0.56	58.71	17.80	5.87	3.7%
3	0.54	51.80	18.62	5.18	3.0%

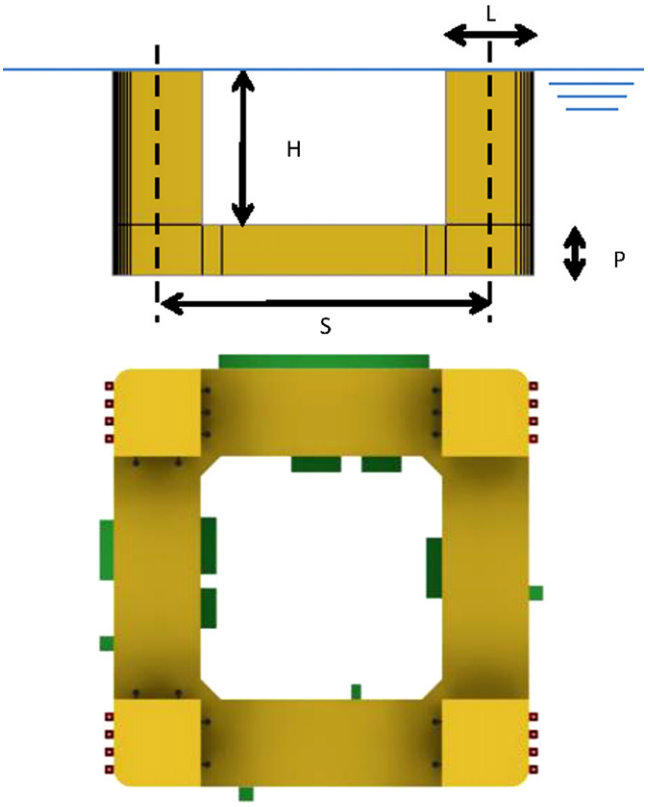

Fig. 2. Characteristic dimensions of a semi-submersible with four square columns.

Fig. 3 shows the coordinate system in 2D horizontal plane. The X and Y axes represent the (basin-fixed) global coordinate system, and x and y are (body-fixed) local coordinate system. In all the tests, the current flow comes from $+X$ QUOTE and $-X$. The current angle of incident, Φ, is defined as the counterclockwise angle from the vector current U to axis x.

The range of current velocities conducted were from 0.03 up to 0.30 m/s that represents a Reynolds number range of 6000 up to 85,000 and a reduced velocity range of $2.50 \leq V_r \leq 20.00$.

The analysis methodology for defining characteristic motion amplitudes was based on a work by Gonçalves et al. (2012a) and can be defined by taking the mean of the 10% largest amplitudes as obtained in the Hilbert–Huang Transform method (HHT), see Huang et al. (1998), both for motions in the transverse and in-line directions, as well as for the yaw motion.

The reduced velocity is defined as:

$$V_r = (U \times T_0)/D \tag{5}$$

where U QUOTE is the incident current velocity, T_0 is the natural period of motion in the transverse direction in still water and D is the characteristic length of the cross-section of the body subjected to a vortex shedding, i.e., $D = \sqrt{2}L$ for 45-degree incidence, where L is the column width.

3.1. Wave tests

The current angle tested was 45-degree incidence, the one presenting highest VIM amplitudes in the transverse direction. At least six different reduced velocities were tested for each condition of simultaneous presence of wave surface and current. Regular and irregular waves (sea conditions) were performed to verify effects on VIM coming from the presence of energy in different frequency ranges.

Three irregular waves, described by a JONSWAP spectra, were chosen to represent different environmental conditions at Campos Basin—Brazil, corresponding to distinct levels of unit motion. Table 2 presents the characteristic parameters of those sea conditions performed, as well as their respective power spectra in Fig. 4.

Five regular waves were chosen to represent different response amplitude operator (RAO) values in the heave motion. The 6 DOF RAO for the semi-submersible are presented in Fig. 5. This methodology was used to verify the wave effects for different vertical motion levels, as commented in Gonçalves et al. (2010b). The regular waves performed are presented in Table 3, in which only the waves with ID from 1 to 3 were carried out with current incidence.

As mentioned, six current velocities were carried out to represent the main reduced velocity range in which the higher transverse VIM was observed, see details in Table 4. It is worth noting that the wave encounter frequency changed due to the current velocity; therefore, the wave encounter frequency was different for each reduced velocity. Nevertheless, these small modifications in frequency did not result in significant changes in the RAO amplitudes. More details about the natural frequencies of the semi-submersible platform tested can be found in Table 5.

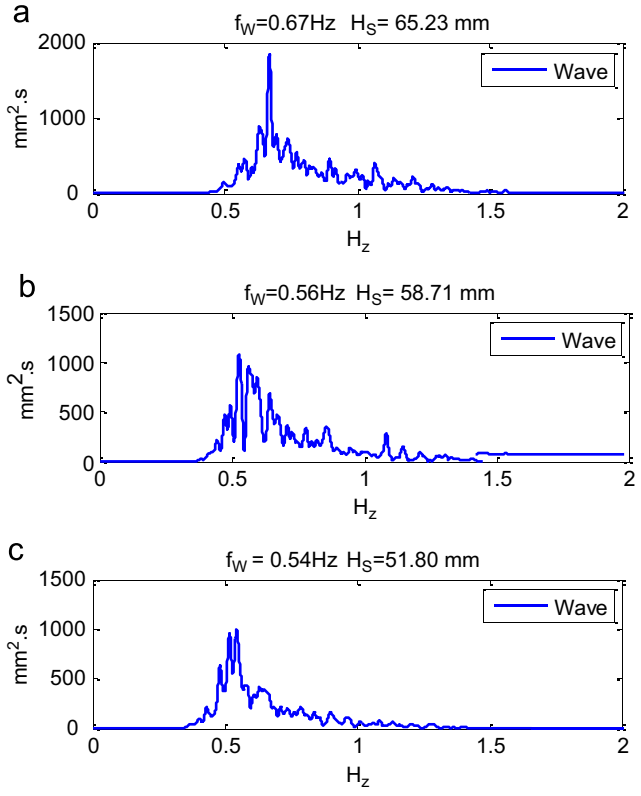

Fig. 4. PSD for JONSWAP sea conditions without current incidence: (a) f_p=0.67 Hz and H_s=65.23 mm, (b) f_p=0.57 Hz and H_s=58.71 mm, and (c) f_P=0.54 Hz and H_S=51.80 mm.

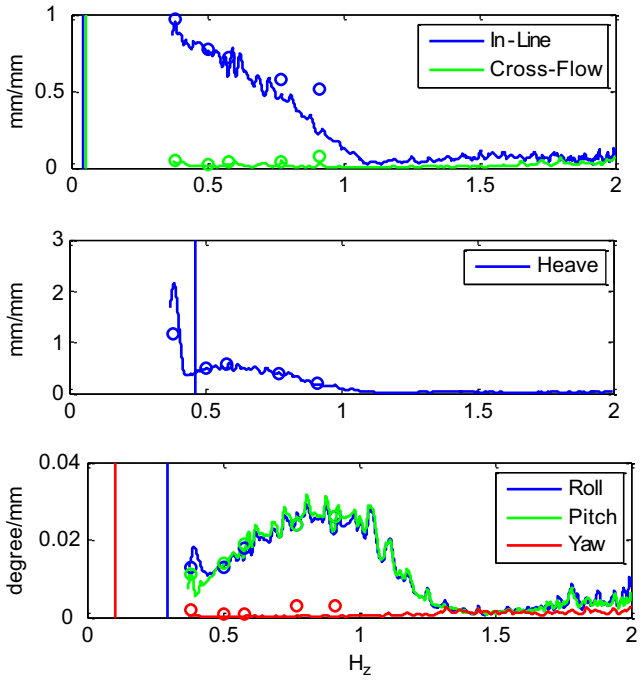

Fig. 5. RAOs for the semi-submersible with four square columns. Lines were obtained from sea condition tests and points by regular wave ones without current incidence.

Table 3
Regular wave characteristics without current incidence.

ID	Model scale–1:100		Full scale–1:1		KA
	f_{RW} [Hz]	H_{RW} [mm]	T_{RW} [s]	H_{RW}[m]	
1	0.91	43.87	10.99	4.39	7.3%
2	0.59	78.91	16.95	7.89	5.5%
3	0.38	116.64	26.32	11.66	3.4%
4	0.77	54.28	12.99	5.43	6.5%
5	0.50	81.66	20.00	8.17	4.1%

Table 4
Current velocities and respective reduced velocities performed (model scale).

Current velocity U [cm/s]	Reduced velocity V_r
6.58	4.28
8.89	5.78
11.19	7.27
13.51	8.78
15.81	10.28
18.12	11.78

Figs. 6 and 7 present examples of time series for a VIM test in the presence of a regular wave and a sea condition, respectively. The time histories of the 6 DOF motions are also presented, as well the wave elevation. The first half of the test comprises only current conditions, in which VIM is well developed. Then, the platform encounters the waves in the second half of the run. The elapsed time for the second half of test is sufficient to observe another different steady state, and then allowing new statistics. In the same figures, power spectra are shown for each DOF obtained for the range with waves, the difference about the wave energy from regular

waves (only one frequency) and sea conditions (a range of frequencies) can be verified.

3.2. Damping tests

A structural set of risers (similar in diameter and positions) was built in the model, however, with length enough only to guarantee the maintenance of coherence in the shedding pattern near the platform and a known increase in the damping. Three different external damping levels were used: the first one represents only the hydrodynamic damping due to the hull; the second and the third ones represent external damping levels higher than the first condition, achieved by including the damping device emulator showed in Fig. 8. The difference between the second and the third external damping levels is the number of 'emulated' risers, i.e., a small number provide lower damping level; these values are described in Table 6. The tests to observe the external damping level effects were carried out for 45-degree incidence. At least 18 different reduced velocities were performed for each test condition.

Table 5
Natural frequencies in still water of the semi-submersible platform in full draft condition (model scale).

Degree of freedom	Natural frequency f_N [Hz]	Natural period T_N [s]
In-line	0.0446	22.44
Transverse	0.0543	18.43
Heave	0.3973	2.52
Roll	0.2934	3.41
Pitch	0.2934	3.41
Yaw	0.1051	9.51

The damping terms can be described as two different forms: linear and quadratic. The linear damping is obtained from the following linear motion equation:

$$(m+m_a)\ddot{y}+b\dot{y}+ky=0 \tag{6}$$

$$\zeta_L=\frac{T_0 b}{4\pi(m+m_a)} \tag{7}$$

where y is the motion in the transverse direction; m structural mass of the platform; m_a is the added mass in the transverse direction; b is the linear damping coefficient; k is the stiffness coefficient; T_0 is the natural period of motion in the transverse direction in still water and ζ_L is the nondimensional linear damping coefficient.

On the other hand, the quadratic damping can be described from the non-linear motion equation:

$$(m+m_a)\ddot{y}+b_1\dot{y}+b_2\dot{y}|\dot{y}|+ky=0, \tag{8}$$

where b_1 is the linear damping coefficient and b_2 is the quadratic damping coefficient. Alternative methods to obtain these coefficients can be found, for example, in Chakrabarti (1994) and Malta et al. (2010).

3.3. Draft tests

Two different load conditions were performed, namely full draft (draft equal to 34 m) and low draft condition (draft equal to 16 m). Fig. 9 shows comparative draws for these configurations and Table 7 presents more details about the submerged areas. The low draft conditions were carried out at 0 and 45-degree

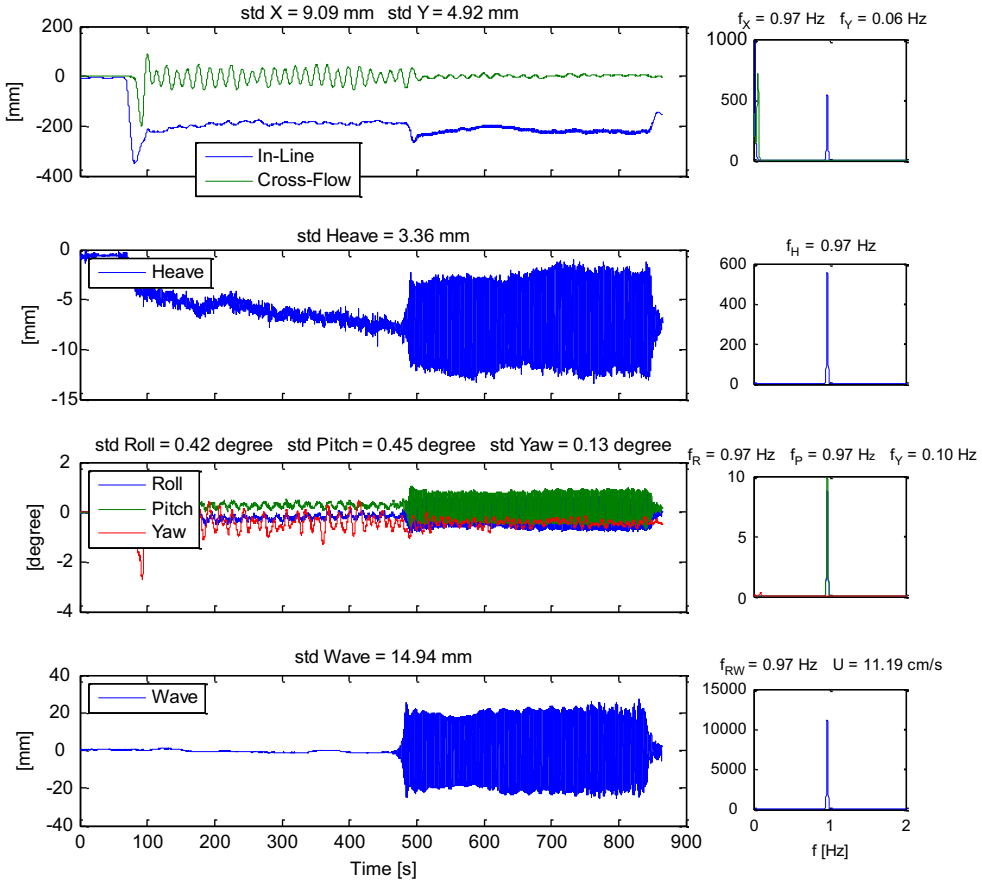

Fig. 6. Six DOF (in-line, transverse, heave, roll, pitch and yaw) and wave elevation for a regular wave (f_{RW}=0.91 Hz and H_{RW}=43.87 mm) and current (U=11.19 cm/s) model test time histories; and power spectrum analyses.

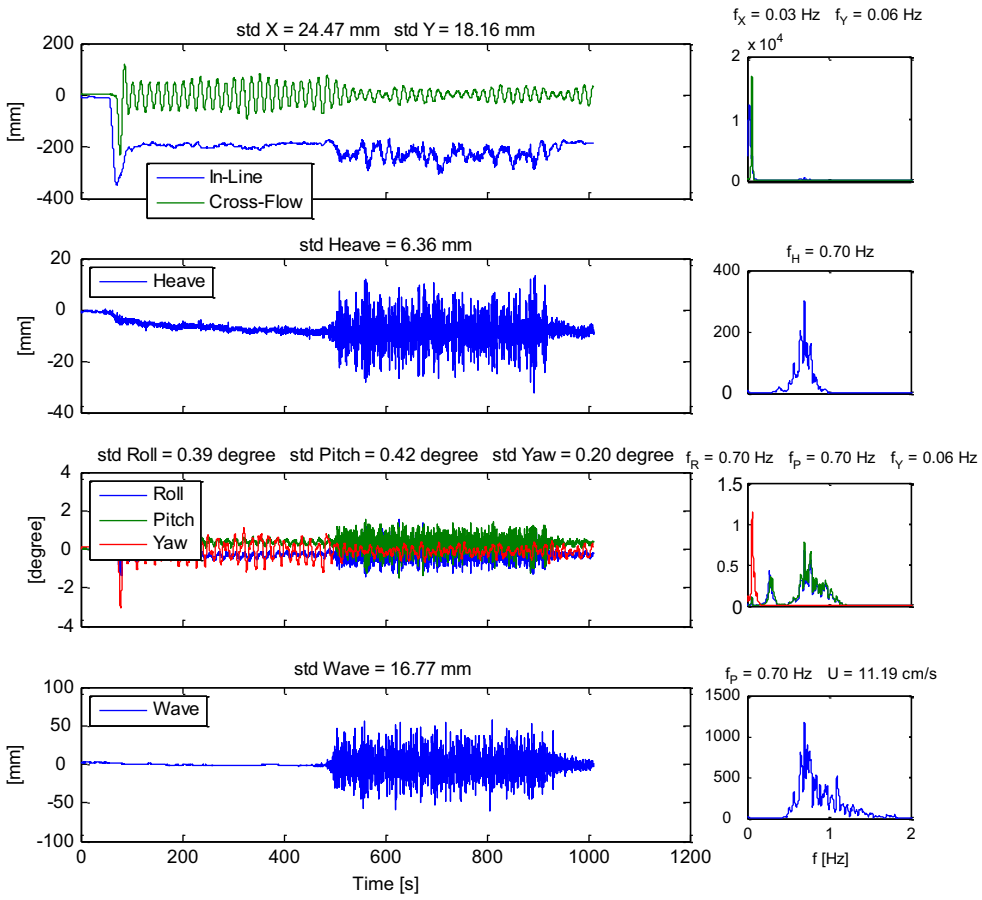

Fig. 7. Six DOF (in-line, transverse, heave, roll, pitch and yaw) and wave elevation for a sea condition (f_p=0.67 Hz and H_S=65.23 mm) and current (U=11.19 cm/s) model test time histories; and power spectrum analyses.

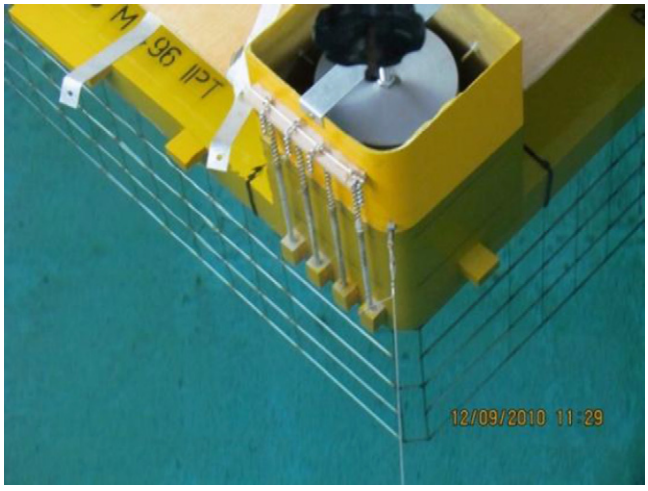

Fig. 8. Picture of the semi-submersible model scaled in 1:100 with external damping simulator.

Table 6
External damping levels.

Condition	ζ_L (%)	b_1	b_2
Without external damping	5.55	1.58	0.69
External damping 1	5.48	1.29	0.81
External damping 2	5.54	1.07	0.85

incidences. At least 18 different reduced velocities were performed for each test condition.

4. Experimental results

4.1. Surface wave effects

Figs. 10 and 11, respectively, present the results of non-dimensional characteristic amplitudes for transverse and the yaw motions. The results are presented for current tests with and without simultaneous wave presence.

According to the results in Fig. 10, the motions in the transverse direction decreased up to 50% with the presence of sea conditions, and they still had a characteristic frequency near the transverse natural frequency, as can be further seen in Fig. 16. Another issue is that the amplitudes were lower for sea conditions with significant higher amplitude. On the other hand, the VIM was mitigated completely in the presence of regular waves, and the motions were similar and very low for the three regular conditions.

The results for yaw amplitudes, in Fig. 11, showed similar behavior, i.e., the yaw motion amplitudes decreased in presence of waves and current, and presented lower amplitudes for regular wave conditions.

Frequency analyses from Power Spectrum Density (PSD) of the motions are also important. Fig. 12 presents the PSD for 45-degree incidence without wave presence, i.e., only in current. The results showed negligible energy in the in-line direction for all frequencies, see Fig. 12a. However, for the motion in the

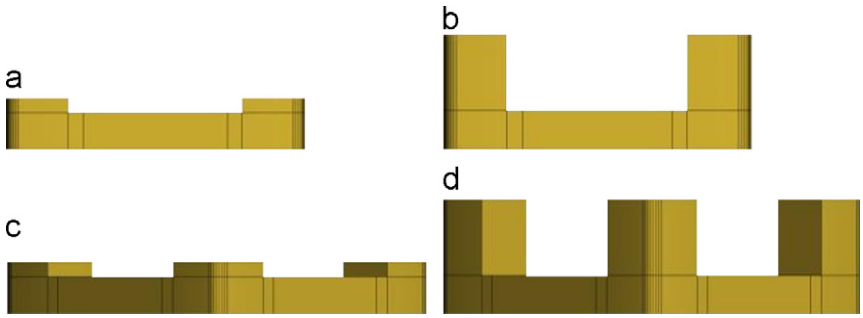

Fig. 9. Submerged projected area for a semi-submersible platform for different incidence angles: (a) $\emptyset=0^\circ$ and low draft condition, (b) $\emptyset=0^\circ$ and full draft condition, (c) $\emptyset=45^\circ$ and low draft condition and (d) $\emptyset=45^\circ$ and full draft condition.

Table 7
Submerged projected area for a semi-submersible for different incidence angles (full scale).

Incidence angle, $\emptyset$	Submerged projected area for a semi-submersible, A_P (m^2)	Aspect ratio of the submerged column portion, *H/L*
0 degree—Full draft	1967.15	1.14
45 degrees—Full draft	3301.88	1.14
0 degree—Low draft	1257.41	0.23
45 degrees—Low draft	1907.05	0.23

transverse direction the energy was presented in the range of reduced velocities $5.0 \leq V_r \leq 9.0$, see Fig. 12b, and for yaw motions in the range of reduced velocities $10.0 \leq V_r \leq 15.0$, see Fig. 12c. It is worth noting that the energy for transverse and yaw motion was concentrated around the natural frequency of the respective DOF, which corroborates the assumption that the VIM is a resonance behavior.

In Figs. 13–18, PSD results for the tests with the simultaneous waves and current are presented to better understand the wave effects on VIM. Figs. 13 and 14 show the PSD results for the motions in the in-line direction; Figs. 15 and 16 for the transverse ones; and, finally, Figs. 17 and 18 for the yaw motions. The results were compared to show the different energy densities present with regular waves and sea conditions.

The greatest differences between them were found in the PSD results for motions in the in-line direction. The energy for this DOF was concentrated in the frequency of the regular waves performed, with no considerable energy in other frequencies, see Fig. 13. Differently, in Fig. 14, the energy density for motion in the in-line direction in the presence of sea condition was higher and concentrated around the natural frequencies of motions on the free surface plane (in-line and transverse, see Table 5). This behavior is known for large-volume semi-submersible, as can be seen, for example, in Matos et al. (2011), denominated second-order motions or specifically slow drift motions, which is a resonant behavior in low frequencies caused by the irregular characteristics of the sea conditions.

PSD for the motions in the transverse direction only confirms that no VIM was evidenced for regular waves, see Fig. 15. At the same time, it confirmed the VIM behavior for sea conditions tests, however, with small amplitudes or small energy density around the transverse natural frequency, as seen in Fig. 16. Moreover, for the yaw motions, Figs. 17 and 18, PSD results showed energy density around yaw natural frequency for both wave tests, but with small energy in the regular ones.

Taking into account the previous results, it is possible to conjecture that the resonance second-order motion in the in-line direction induced by the sea condition incidence did not mitigate the VIM completely, differently from the regular wave incidence.

The in-line motion due to the wave excitation can be considered as the imposed oscillatory motion and the respective Keulegan–Carpenter number calculated using Eq. (1), for regular waves, and Eq. (3) for sea condition incidence. The effect of simultaneous current and waves is calculated using the ratio α as in Eq. (4). The region of either drag or inertia force for the tests with simultaneous wave surface and current can be seen in the plot α vs. *KC*, see Fig. 19, as proposed in Iwagaki and Asano (1984). The limit curve represents the condition in which the drag force (viscous) is equal to the inertia force, being calculated as:

$$KC = \frac{1+C_a}{C_D}(\pi\alpha)^2, \tag{9}$$

where C_a is the transverse (or in-line) added mass of the platform for 45-degree incidence and C_D is the static drag coefficient for 45-degree incidence. The values of these coefficients for the semi-submersible under study are $C_a \cong 0.76$ and $C_D \cong 0.75$.

The results presented in Fig. 19 showed that the regular and sea state conditions were in distinct behavior regions, predominant inertia and predominant drag (viscous), respectively. It is possible to infer that the VIM existence probably depends on the imposed in-line motions due to the wave incidences to be at the predominantly drag (viscous) region, where the viscous or lift forces due to vortex shedding are considerable. The fact that VIM was not verified for regular wave tests is justified because imposed in-line motions due to regular waves were located at the predominant inertia region, i.e., the behavior in which the inertia forces are greater than the forces due to vortex shedding.

The same procedure was applied to the results presented in Gonçalves et al. (2010b) for a monocolumn platform subjected to current and regular wave incidence. Even for regular waves, the monocolumn platform experimented VIM lower than with current incidence only, differently from the semi-submersible platform; however, the imposed in-line motion due to wave was located at the predominantly drag (viscous) force, as can be seen in Fig. 20, in which VIM can be verified.

The in-line response due to waves may be conjectured as the one responsible for the possible VIM existence, rather than the wave nature (regular or irregular). However, the VIM amplitude also depends on the motion amplitudes of the other DOF, mainly heave, roll and pitch; as first discussed in Gonçalves et al. (2010b).

This behavior needs to be further studied, mainly through fundamental tests with cylinders subjected to current and forced to oscillate in the in-line direction simultaneously, and with cylinders free to oscillate due to a more complete set of currents and waves. This kind of investigation has been performed by the authors in order to complement the assumptions made herein.

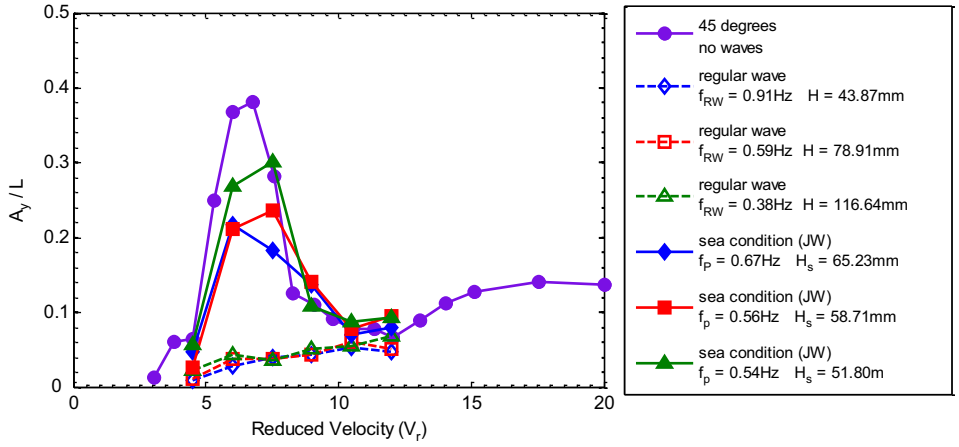

Fig. 10. Nondimensional amplitudes for the motions in the transverse direction for 45-degree current incidence: regular waves, sea conditions and without wave incidence.

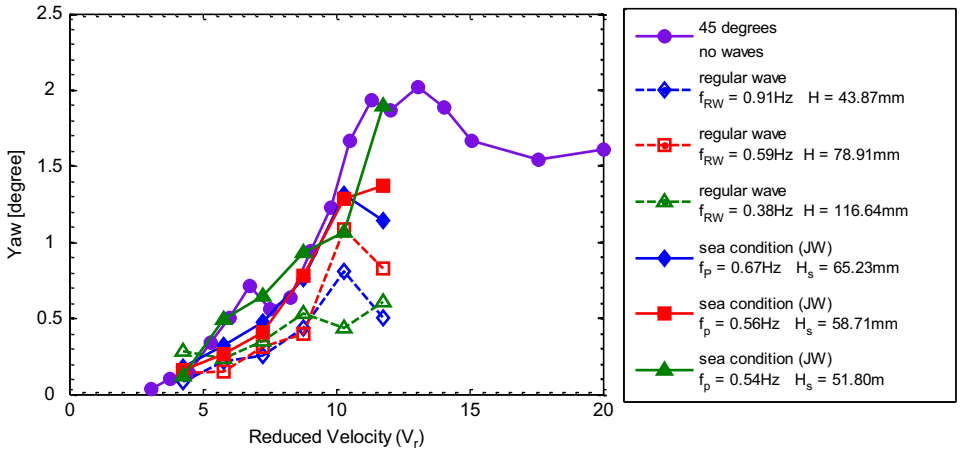

Fig. 11. Yaw characteristic amplitudes for 45-degree current incidence: regular waves, sea conditions and without wave incidence.

4.2. Damping level effects

The presence of risers and mooring lines increased the damping of the system, which reduced the VIM amplitudes, as can be seen in Fig. 21 and Fig. 22, respectively. The results showed lower amplitudes for higher external damping levels (or higher dissipative forces), mainly for transverse motions. In Fig. 22, the yaw amplitude differences between the cases with and without external damping were small due to the small difference in the damping level for this DOF. The increase in the external damping was promoted by the increase in the quadratic component in the non-linear motion equation, b_2; see Eq. (8) and Table 6. As also speculated in Gonçalves et al. (2010b), such effect may be caused partly by the presence of the risers related to the changes in the flow surroundings the platform, which may have been more influenced by tridimensional effects.

The quadratic component of damping is related to drag forces, which is important for maximum tensions in risers and mooring lines. In Figs. 23 and 24, the results of drag coefficient force for the external damping levels are presented. The increase of drag force coefficient can be related with the increase of damping. In turn, the lift force coefficient decreased with the increase of damping, see Fig. 25, which is coherent with the low motion amplitudes verified.

4.3. Draft condition effects

Similarly to Waals et al. (2007) and Gonçalves et al. (2010b), the draft condition was the aspect that had greater effect on VIM amplitudes. A complete attenuation on VIM was noted in the results presented in Fig. 25 and Fig. 26, at 0 and 45-degree incidences. The decrease in amplitudes was correlated with the small immersed length of the platform columns, which does not provide a regular vortex shedding in the water surface plane capable of promoting oscillating excitation forces, thus VIM. The major portion of the platform exposed to flow incidence in low draft condition is the pontoon region, which causes more tridimensional effects on the problem; effects that can be added by using blister in this type of platform, as reported by Xu (2011) and Xu et al. (2012), and therefore reducing VIM. But the blister solution has a problem; the increase in drag force levels may be more harmful to risers and mooring lines fatigue life than the oscillatory tension due to VIM, making the solution sometimes unfeasible.

5. Conclusions

Although the VIM of semi-submersibles is quite important in the design of risers and mooring line systems, the VIM behavior

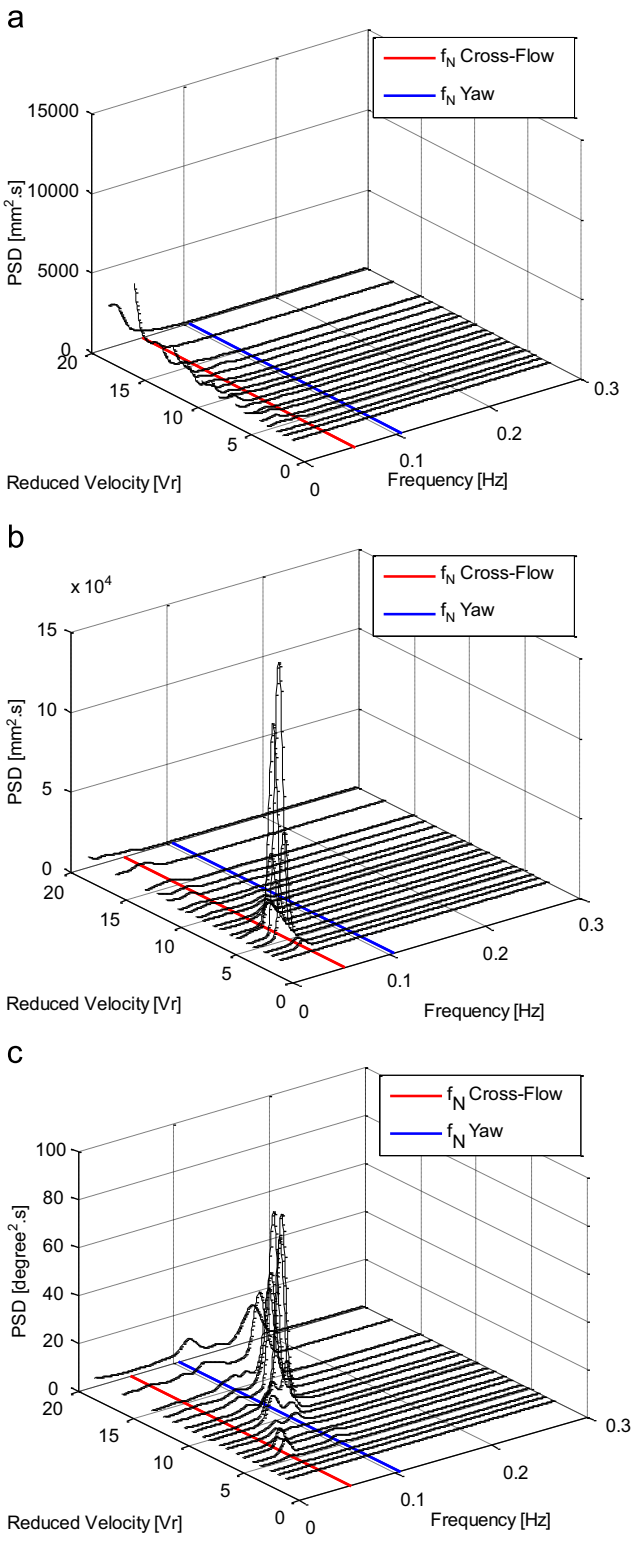

Fig. 12. PSD for 45-degree current incidence angle without waves for the motions: (a) in-line direction, (b) transverse direction, and (c) yaw.

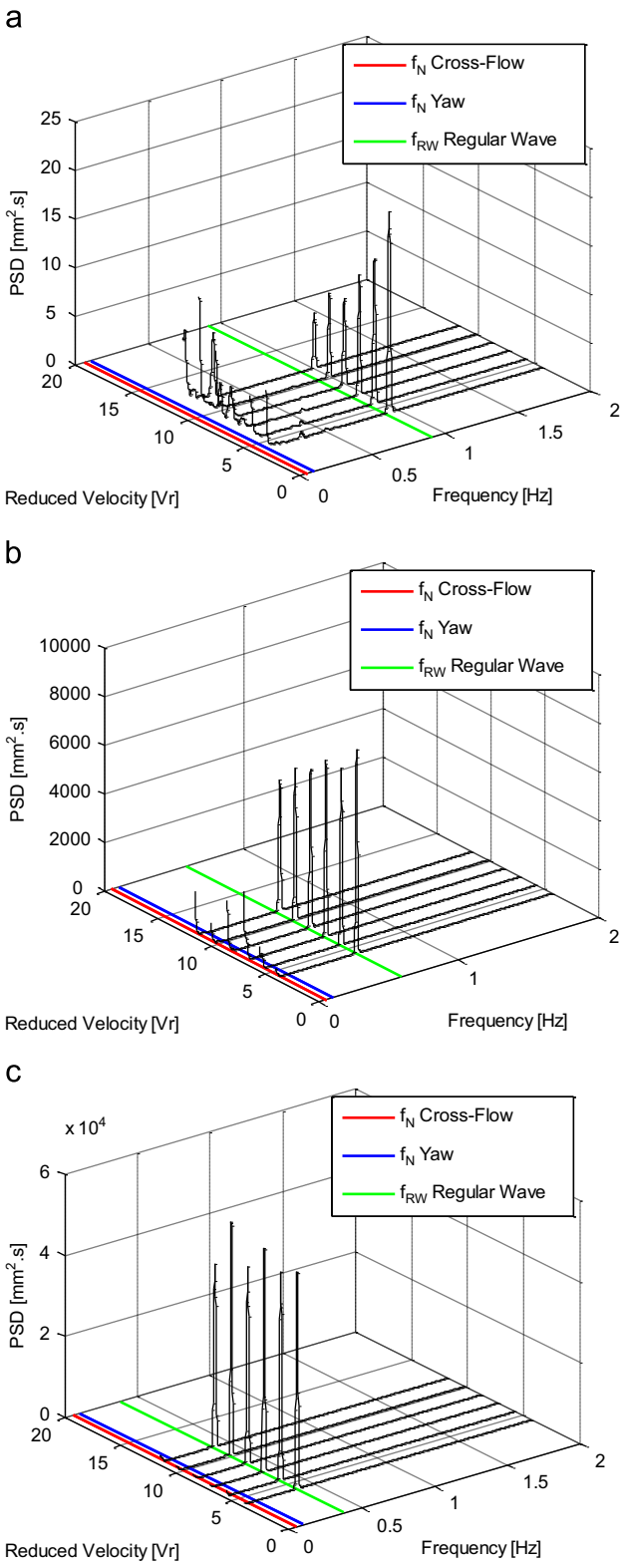

Fig. 13. PSD for the motions in the in-line direction for three different regular waves and current simultaneously: (a) f_{RW}=0.91 Hz and H=43.87 mm, (b) f_{RW}=0.59 Hz and H=78.91 mm, and (c) f_{RW}=0.38 Hz and H=116.64 mm.

with simultaneous presence of current and waves, effects of external damping and different draft conditions have not been thoroughly studied yet. This paper addresses these issues.

The VIM small-scale (1:100) model tests performed on a semi-submersible with four square columns at the Institute of Technological Research (IPT), Brazil are herein reported. The tests aimed to complete the work by Gonçalves et al. (2012d) investigating the effects of the simultaneous presence of wave surface and current incidence in the same direction, i.e., regular waves with energy distributed in a narrow range of frequency (theoretically only one frequency) and JONSWAP sea conditions, in which the energy is distributed in a range of frequencies;

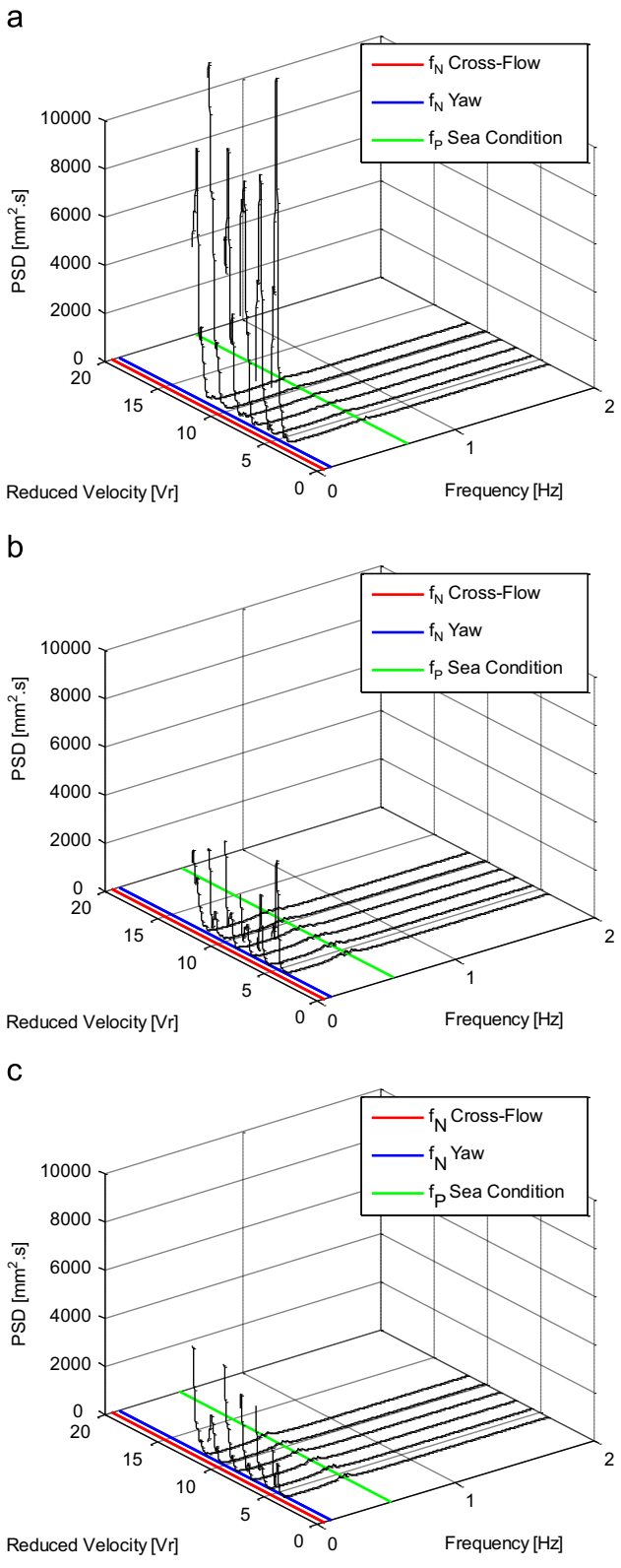

Fig. 14. PSD for the motions in the in-line direction for three different sea conditions and current simultaneously: (a) $f_P = 0.67$ Hz and $H_S = 65.23$ mm, (b) $f_P = 0.56$ Hz and $H_S = 58.71$ mm, and (c) $f_P = 0.54$ Hz and $H_S = 51.80$ mm.

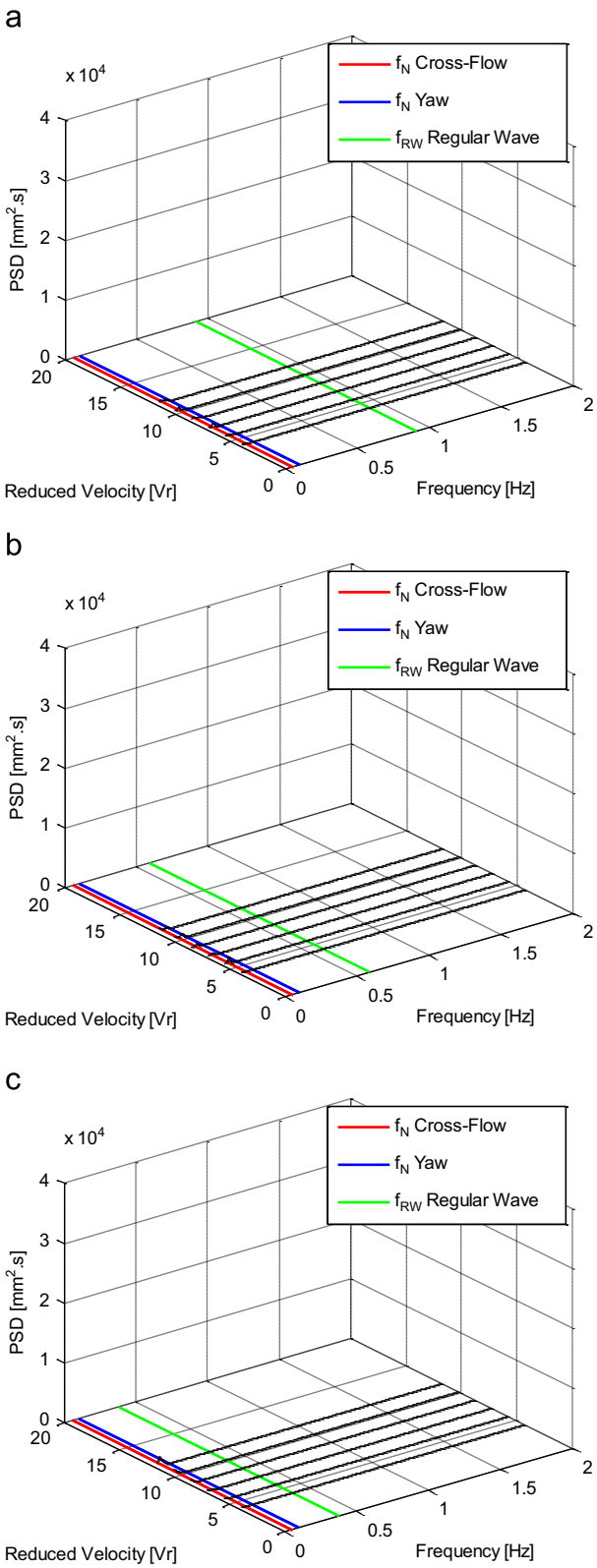

Fig. 15. PSD for the motions in the transverse direction for three different regular waves and current simultaneously: (a) $f_{RW} = 0.91$ Hz and $H = 43.87$ mm, (b) $f_{RW} = 0.59$ Hz and $H = 78.91$ mm, and (c) $f_{RW} = 0.38$ Hz and $H = 116.64$ mm.

external damping level due to the presence of 'emulated' risers and mooring lines; and draft conditions. The main results discussed comply with motions in the transverse and in-line direction, as well as yaw motion and the conclusions reached are as follows.

The results showed that, in regular wave tests, the VIM was completely mitigated. Motions in the transverse direction were not observed and the energy around the natural frequency of transverse motions could not be found. Moreover, smaller yaw

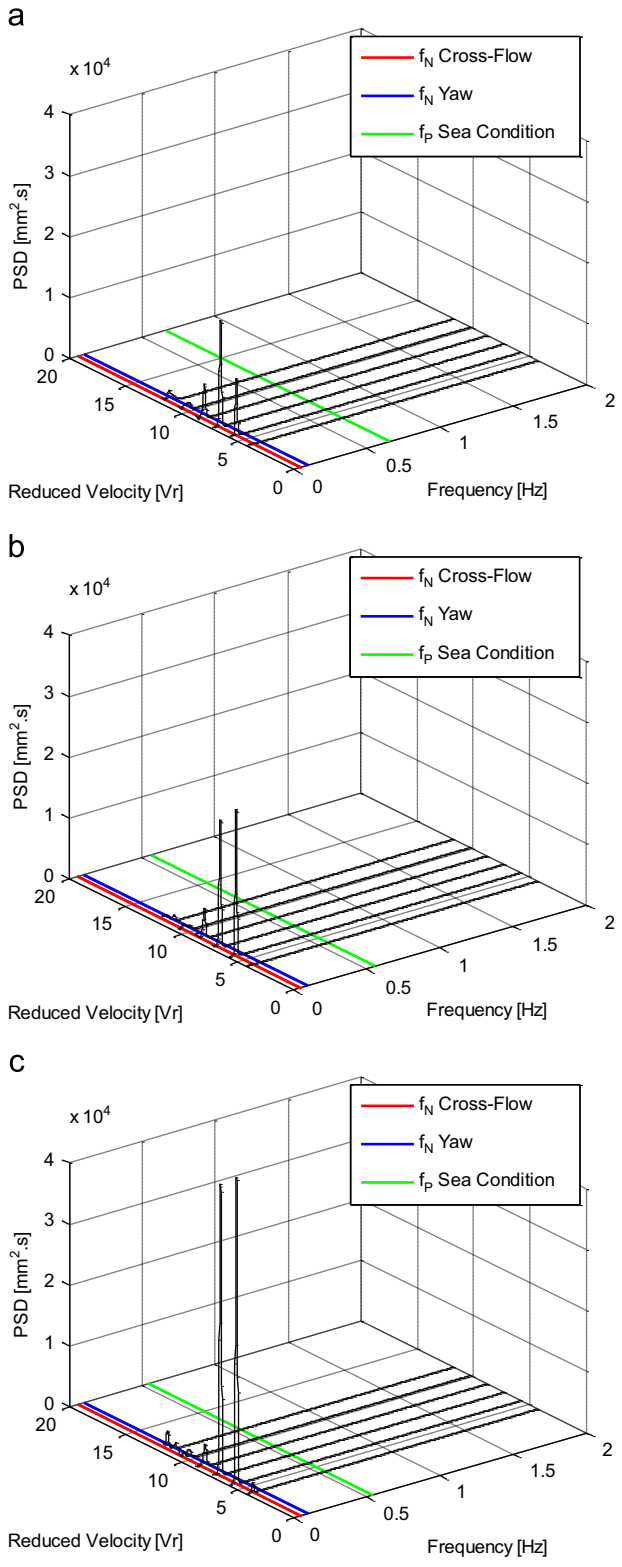

Fig. 16. PSD for the motions in the transverse direction for three different sea conditions and current simultaneously: (a) f_p=0.67 Hz and H_S=65.23 mm, (b) f_p=0.56 Hz and H_S=58.71 mm, and (c) f_P=0.54 Hz and H_S=51.80 mm.

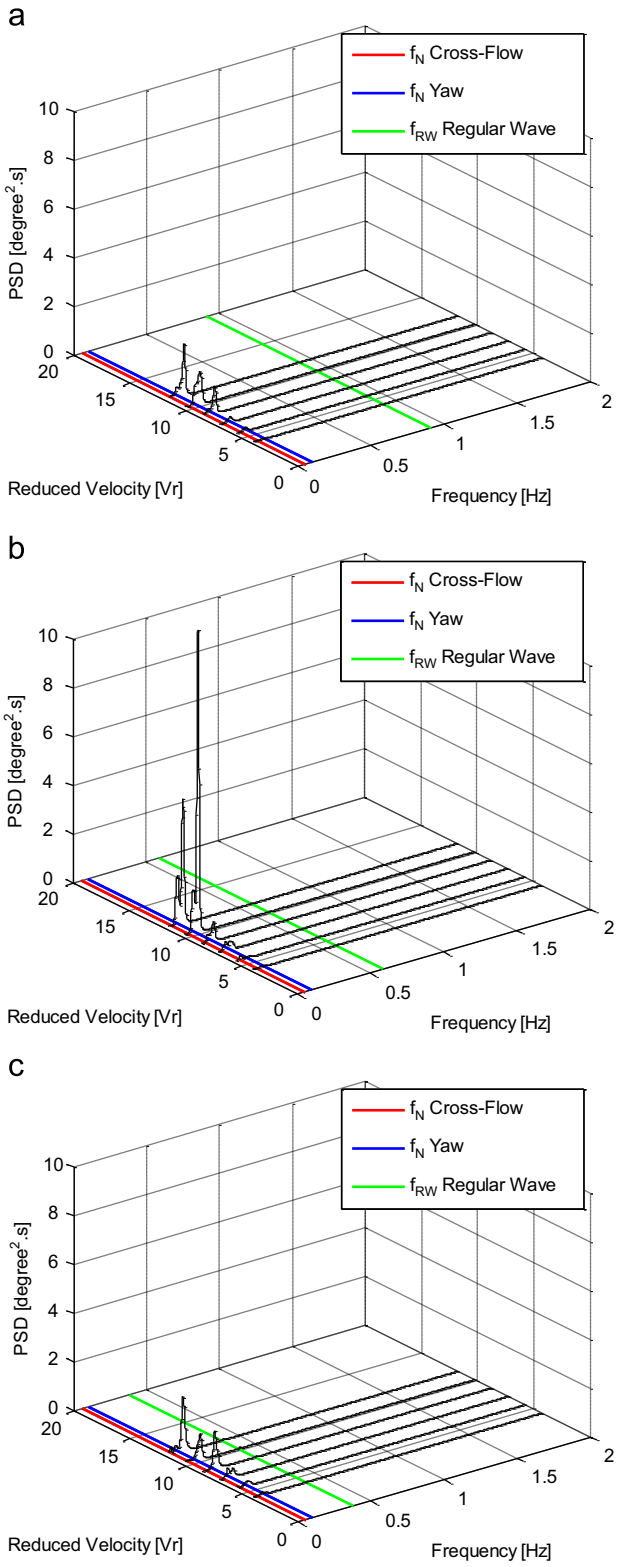

Fig. 17. PSD for yaw motions for three different regular waves and current simultaneously: (a) f_{RW}=0.91 Hz and H=43.87 mm, (b) f_{RW}=0.59 Hz and H=78.91 mm, and (c) f_{RW}=0.38 Hz and H=116.64 mm.

motion amplitudes were observed when compared with the case without wave incidences. Differently, the results for the sea condition tests showed lower VIM when compared with the case without waves, but the PSD showed considerable energy levels around the natural frequency of motions, transverse and yaw.

The authors speculated that the VIM amplitudes depend on the in-line motions imposed by the incident waves in the platform. This behavior is better understood by making plot α vs. KC using the in-line motions due to waves as the imposed oscillatory motion. In the sea condition tests, the resonance second-order

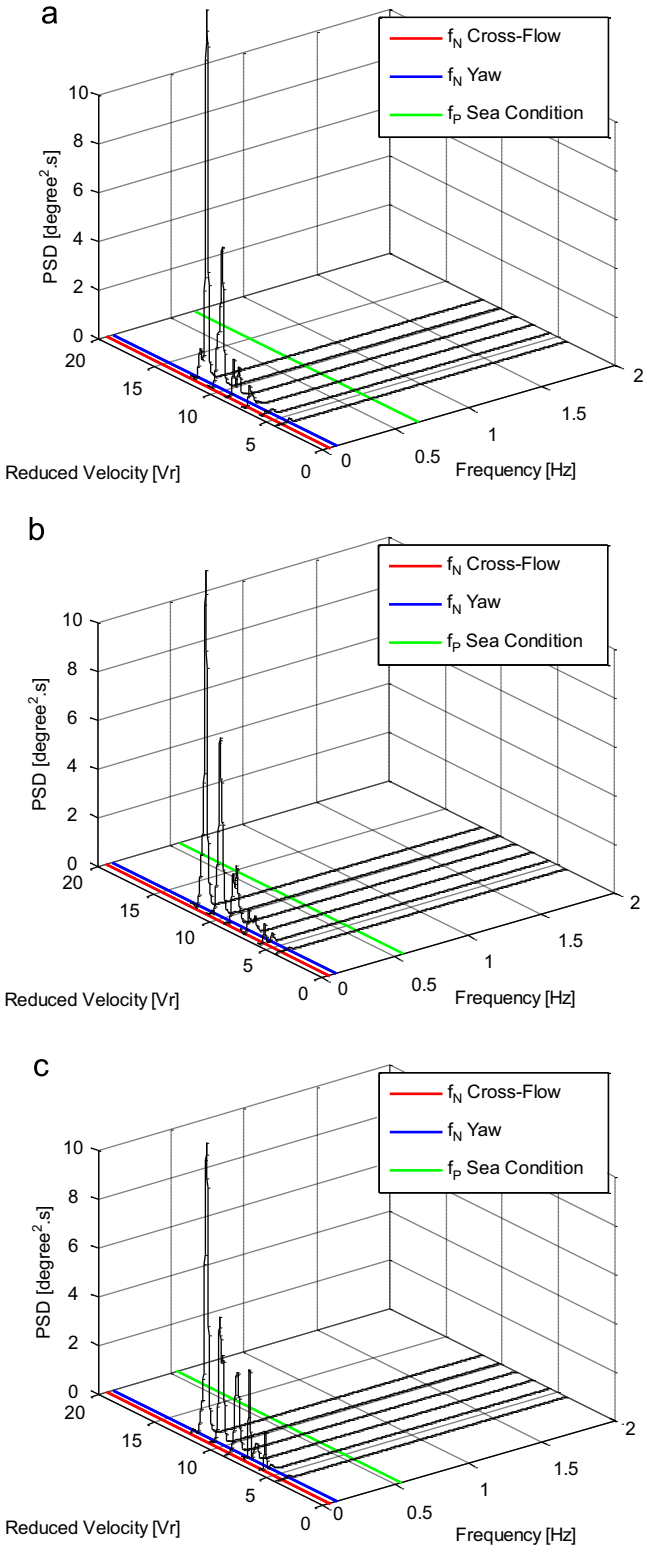

Fig. 18. PSD for yaw motions for three different sea conditions and current simultaneously: (a) f_p=0.67 Hz and H_S=65.23 mm, (b) f_p=0.56 Hz and H_S=58.71 mm, and (c) f_P=0.54 Hz and H_S=51.80 mm.

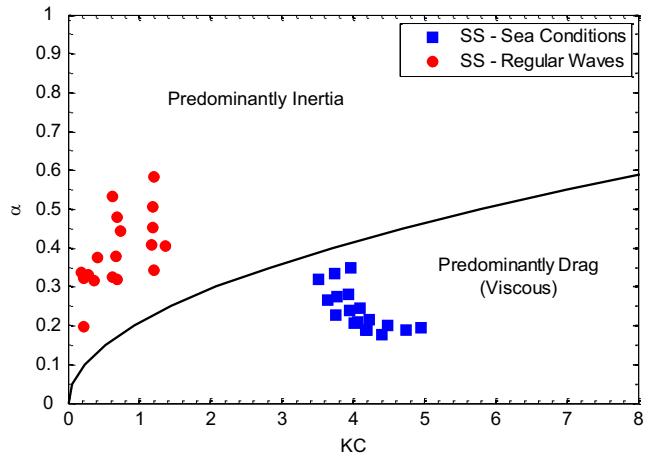

Fig. 19. Predominant region of either drag or inertia force using the in-line motion as the imposed oscillatory motion due to wave incidences for the semi-submersible platform.

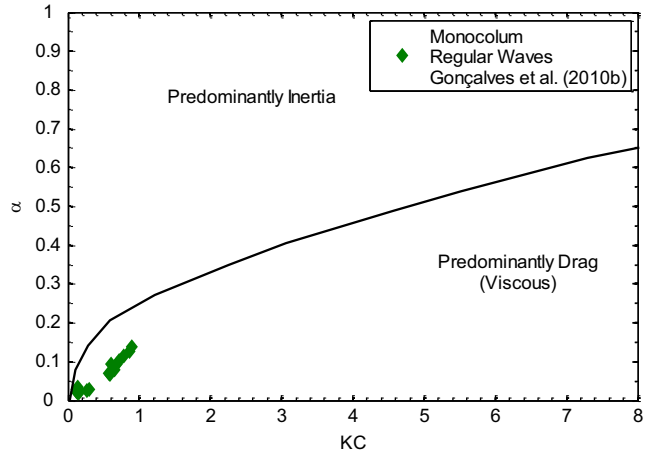

Fig. 20. Predominant region of either drag or inertia force using the in-line motion as the imposed oscillatory motion due to wave incidences for the monocolum platform [Gonçalves et al. (2010b)].

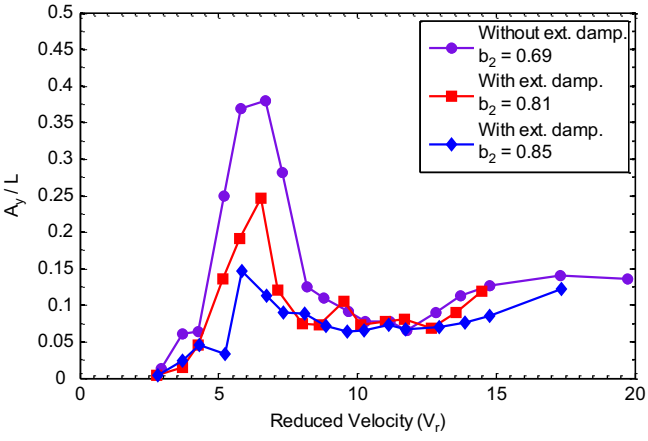

Fig. 21. Nondimensional amplitudes for the motions in the transverse direction for 45-degree incidence: different external damping levels.

motion in the in-line direction occurred, and then the motions in the in-line direction were predominantly in the in-line natural frequency of the system. Conversely, the regular wave characteristics provided in-line motions in the excitation frequency. Using these results, the velocity ratio α for the regular wave incidence was located at the predominantly inertia region, where the forces due to the vortex shedding are small and the VIM does not occur; however, the sea condition incidences were located at the predominantly drag (viscous) region, where the forces due to vortex

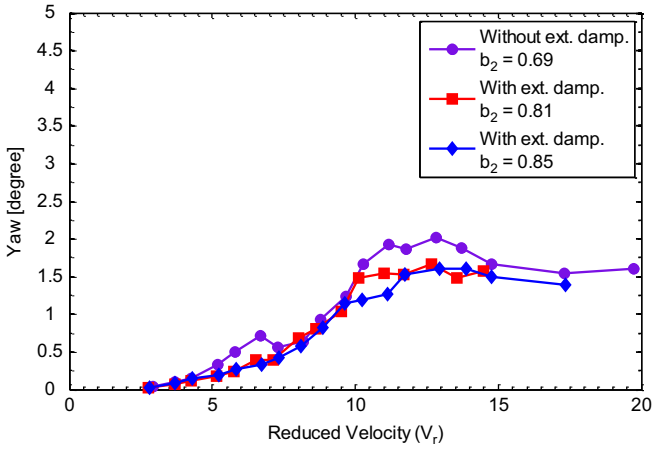

Fig. 22. Yaw characteristic amplitudes for 45-degree incidence: different external damping levels.

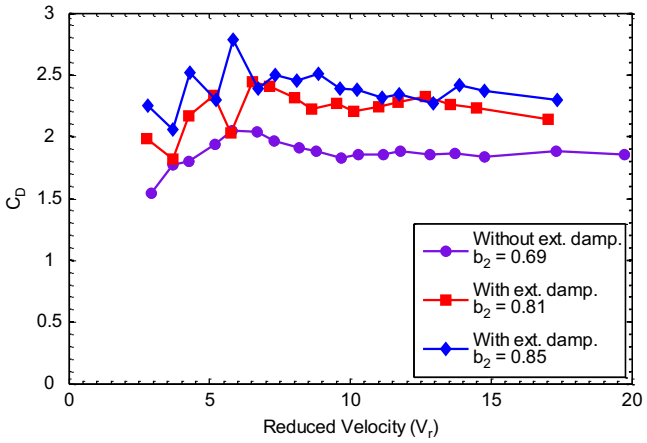

Fig. 23. Drag force coefficient for 45-degree incidence: different external damping levels. The coefficient was obtained using the corresponding submerged projected area, A_P for 45-degree incidence.

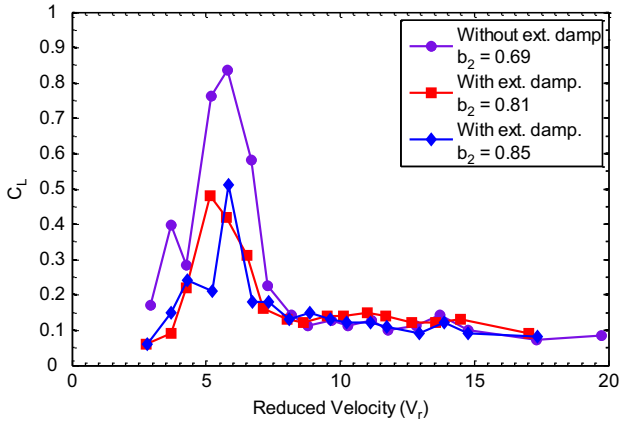

Fig. 24. Lift force coefficient for 45-degree incidence: different external damping levels. The coefficient was obtained using the corresponding submerged projected area, A_P for 45-degree incidence.

shedding are significant and VIM may occur, and the VIM amplitudes also depend on the heave, roll and pitch motions. This assumption must be confirmed with more tests and studied in depth with fundamental experiments on simplified geometries such as bare cylinders, which has been done by the authors.

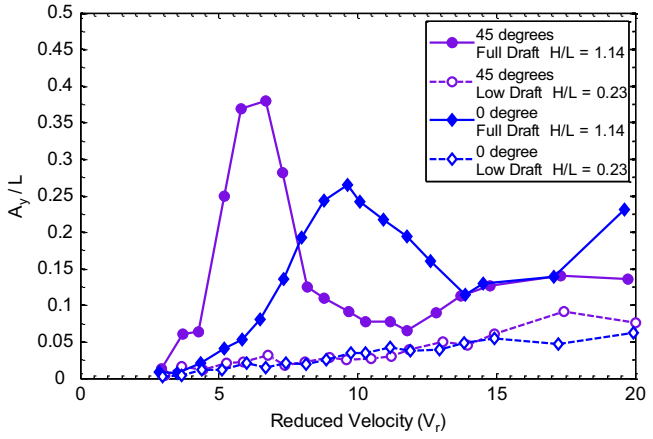

Fig. 25. Nondimensional amplitudes for the motions in the transverse direction for 0 and 45-degree incidences: different draft conditions.

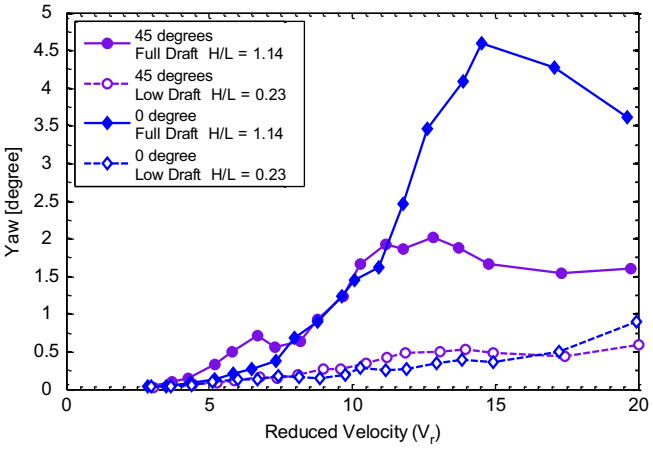

Fig. 26. Yaw characteristic amplitudes for 0 and 45-degree incidences: different draft conditions.

The results showed an amplitude decrease around 50% with the increase in the external damping level around 20%, but still with a determined oscillation frequency. The experiment reported a drag force increase with 'emulated' risers, which are not good for maximum tension levels.

Moreover, the low draft condition (lower exposed portion of the columns) completely attenuated the VIM, i.e., motion amplitudes and dominant frequencies were not verified. In the low draft condition, the lift forces due to vortex shedding are not sufficient to promote VIM, due to the large tridimensional effects promoted around columns and pontoons connections.

The aspects studied here, together with those presented in Part I, showed to be decisive in the VIM behavior, needing to be considered in the design phase, not only for risers and mooring lines definition, but also for the hull definition.

Acknowledgements

The authors thank Petrobras for the help in performing the tests. We also thank the IPT and Oceânica Offshore–Brazil personnel, in particular, Eng. MSc. Marcos Cueva, for their efforts during the test campaign. Prof. Dr. André L. C. Fujarra presents his gratitude to the support provided by the Brazilian Navy and by the Maritime Research Institute Netherlands during his sabbatical year, period in which this work was completed. The authors thank Prof. Dr. Celso P. Pesce and Prof. Dr. Kazuo Nishimoto for

their help in the discussions. We would also like to acknowledge FAPESP and CAPES for the financial support.

References

Blevins, R.D., Coughran, C.S., 2009. Experimental investigation of vortex-induced vibration in one and two dimensions with variable mass, damping, and Reynolds number. J. Fluids Eng. 131 101202-1.

Borthwick, A.G.L., Herbert, D.M., 1988. Loading and response of a small diameter flexibly mounted cylinder in waves. J. Fluids Struct. 2, 479–501.

Chakrabarti, S.K., 1994. Offshore structure modeling. Adv. Ser. Ocean Eng. 9, 445–451.

Cueva, M., Fujarra, A.L.C., Nishimoto, K., Quadrante, L., Costa A. 2006 Vortex induced motion: model testing of a monocolumn floater. In: Proceedings of the 25th International Conference on Offshore Mechanics and Arctic Engineering. Hamburg, Germany: OMAE2006-92167.

DNV 2007. Recommended Practice DNV-RP-C205–Environmental Conditions and Environmental Loads. April 2007.

DNV 2008. Offshore Standard DNV-OS-E301–Position Mooring. October 2008.

Faltinsen, O., 1994. Wave and current induced motions of floating production systems. Appl. Ocean Res. 15, 351–370.

Finnigan, T., Irani, M., van Dijk, R. 2005. Truss SPAR VIM in waves and currents. In: Proceedings of the 24th International Conference on Offshore Mechanics and Arctic Engineering. Halkidiki, Greece. OMAE2005-67054.

Fox, T.A., Apelt, C.J., 1993. Fluid-induced loading of cantilevered circular cylinders in a low-turbulence uniform flow. Part 3: Fluctuating loads with aspect ratios 4 to 25. J. Fluids Struct. 7, 375–386.

Fujarra, A.L.C., Rosetti, G.F., De Wild, J., Gonçalves, R.T.. 2012. State-of-art on vortex-induced motion: a comprehensive survey after more than one decade of experimental investigation. In: Proceedings of the 31st International Conference on Ocean, Offshore and Arctic Engineering. Rio de Janeiro, Brazil: OMAE2012-83561.

Gonçalves, R.T., Franzini, G.R., Fujarra, A.L.C., Meneghini, J.R. 2010a. Two degrees-of-freedom vortex-induced vibration of a circular cylinder with low aspect ratio. In: Proceedings of BBVIV-6 Bluff Body Wakes and Vortex-Induced Vibrations. Capri Island, Italy.

Gonçalves, R.T., Fujarra, A.L.C., Rosetti, G.F., Nishimoto, K., 2010b. Mitigation of vortex-induced motion (VIM) on a monocolumn platform: forces and movements. J. Offshore Mech. Arct. Eng. 132 (4), 041102.

Gonçalves, R.T., Franzini, G.R., Rosetti, G.F., Fujarra, A.L.C., Nishimoto, K., 2012a. Analysis methodology for vortex-induced motions (VIM) of a monocolumn platform applying the Hilbert–Huang transform method. J. Offshore Mech. Arct. Eng. 134 (1), 011103.

Gonçalves, R.T., Rosetti, G.F., Fujarra, A.L.C., Freire, C.M., Franzini, G.R., Meneghini, J.R., 2012b. Experimental comparison of two degrees-of-freedom vortex-induced vibration on high and low aspect ratio cylinders with small mass ratio. J. Vib. Acoust. 134 (6), 061009.

Gonçalves, R.T., Rosetti, G.F., Fujarra, A.L.C., Nishimoto, K., 2012c. An overview of relevant aspects on VIM of spar and monocolumn platforms. J. Offshore Mech. Arct. Eng. 134 (1), 014501.

Gonçalves, R.T., Rosetti, G.F., Fujarra, A.L.C., Oliveira, A.C., 2012d. Experimental study on vortex-induced motions of a semi-submersible platform with four square columns, Part I: Effects of current incidence angle and hull appendages. Ocean Eng. 54, 150–169.

Hong, Y., Choi, Y., Lee, J., Kim, Y. 2008. Vortex-induced motion of a deep-draft semi-submersible in current and waves. In: Proceedings of the 18th International Offshore and Polar Engineering Conference. Vancouver, BC, Canada.

Huang, N.E., Shen, Z., Long, S.R., Wu, M.C., Shih, H.H., Zheng, Q., Yen, N.-C., Tung, C.C., Liu, H.H., 1998. The empirical mode decomposition and the Hilbert spectrum for nonlinear and non-stationary time series analysis. Proc. R. Soc. London, Ser. A, 903–995.

Hussain, A., Nah, E., Fu, R., Gupta, A. 2009 Motion comparison between a conventional deep draft semi-submersible and a dry tree semi-submersible. In: Proceedings of the 28th International Conference on Ocean, Offshore and Arctic Engineering. Honolulu, Hawaii, USA: OMAE2009-80006.

Irani, M., Finn, L. 2005 Improved strake design for vortex induced motions of spar platforms. In: Proceedings of the 24th International Conference on Offshore Mechanics and Arctic Engineering. Halkidiki, Greece: OMAE2005-67384.

Iwagaki, Y., Asano, T. 1984. Hydrodynamic forces on a circular cylinder due to combined wave and current loading. In: Proceedings of the International Conference on Coastal Engineering, No. 19.

Jauvtis, N., Williamson, C.H.K., 2004. The effect of two degrees of freedom on vortex-induced vibration at low mass and damping. J. Fluid Mech. 509, 23–62.

Klamo, J.T., Leonard, A., Roshko, A., 2006. The effects of damping on the amplitude and frequency response of a freely vibrating cylinder in cross-flow. J. Fluids Struct. 22, 845–856.

Kozakiewicz, A., Sumer, B.M., FredsØe, J., 1994. Cross-flow vibrations of cylinder in irregular oscillatory flow. J. Waterw. Port Coastal Ocean Eng. 120, 515–534.

Magee, A., Sheikh, R., Guan, K.Y.H., Choo, J.T.H., Malik, A.M.A., Ghani, M.P.A., Abyn, H. 2011. Model tests for VIM of multi-column floating platforms. In: Proceedings of the 29th International Conference on Ocean, Offshore and Arctic Engineering. Rotterdam, The Netherlands: OMAE2011-49151.

Malta, E.B., Gonçalves, R.T., Matsumoto, F.T., Pereira, F.R., Fujarra, A.L.C., Nishimoto, K. 2010. Damping coefficient analyses for floating offshore structures. In: Proceedings of the 29th International Conference on Offshore Mechanics and Arctic Engineering. Shanghai, China. OMAE2010-20093.

Martin, B., Rijken, O. 2012. Experimental analysis of surface geometry, external damping and waves on semisubmersible vortex induced motions. In: Proceedings of the 31st International Conference on Ocean, Offshore and Arctic Engineering. Rio de Janeiro, Brazil: OMAE2012-83689.

Matos, V.L.F., Simos, A.N., Sphaier, S.H., 2011. Second-order resonant heave, roll and pitch motions of a deep-draft semi-submersible: theoretical and experimental results. Ocean Eng. 38, 2227–2243.

Morse, T.L., Govardhan, R.N., Williamson, C.H.K., 2008. The effect of end conditions on the vortex-induced vibration of cylinder. J. Fluids Struct. 24, 1227–1239.

Moureau, F., Huang, S. 2010. Model testing on cross-flow vortex-induced vibration in combined in-line and oscillatory flows. In: Proceedings of the 29th International Conference on Offshore Mechanics and Arctic Engineering. Shanghai, China. OMAE2010-20934.

Rijken, O., Leverette, S., Davies, K. 2004. Vortex induced motions of semi submersible with four square columns. In: Proceedings of the 16th Deep Offshore Technology Conference and Exhibition. New Orleans, Louisiana, USA.

Rijken, O., Leverette, S. 2008. Experimental study into vortex induced motion response of semi submersible with square columns. In: Proceedings of the 27th International Conference on Offshore Mechanics and Arctic Engineering. Estoril, Portugal: OMAE2008-57396.

Rijken, O., Schuurmans, S., Leverette, S. 2011. Experimental investigation into the influences of SCRs and appurtenances on deepdraft semisubmersible vortex induced motion response. In: Proceedings of the 30th International Conference on Ocean, Offshore and Arctic Engineering. Rotterdam, The Netherlands: OMAE2011-49365.

Saito, M., Masanobu, S., Taniguchi, T., Otsubo, K., Asanuma, T., Maeda, K. 2012. Experimental evaluation of VIM on MPSO in combined environmental conditions for waves and current. In: Proceedings of the 31st International Conference on Ocean, Offshore and Arctic Engineering. Rio de Janeiro, Brazil: OMAE2012-83283.

Sarpkaya, T., Isaacson, M., 1981. Mechanics of Wave Forces on Offshore Structures. Van Nostrand Reinhold, New York, pp. 319–322.

Someya, S., kuwabara, J., Li, Y., Okamoto, K., 2010. Experimental investigation of a flow-induced oscillating cylinder with two degrees-of-freedom. Nucl. Eng. Des. 240, 4001–4007.

Sumer, B.M., FredsØe, J., 1988. Transverse vibration of an elastically mounted cylinder exposed to an oscillating flow. J. Offshore Mech. Arct. Eng. 110, 387–394.

Tahar, A., Finn, L. 2011. Vortex induced motion (VIM) performance of the multi column floater (MCF)—drilling and production unit. In: Proceedings of the 29th International Conference on Ocean, Offshore and Arctic Engineering. Rotterdam, The Netherlands: OMAE2011-50347.

Tung, C.C., Huang, N.E., 1973. Combined effects of current and waves on fluid force. Ocean Eng. 2, 183–193.

Van Dijk, R.R., Magee, A., Perryman, S., Gebara, J. 2003. Model test experience on vortex induced vibrations of truss spars. In: Proceedings of the Offshore Technology Conference (OTC 2003), Houston, USA. OTC2003-15242.

Waals, O.J., Phadke, A.C., Bultema, S. 2007. Flow induced motions of multi column floaters. In: Proceedings of the 26th International Conference on Offshore Mechanics and Arctic Engineering. San Diego, California, USA: OMAE2007-29539.

Xu, Q. 2011. A new semisubmersible design for improved heave motion, vortex-induced motion and quayside stability. In: Proceedings of the 29th International Conference on Ocean, Offshore and Arctic Engineering. Rotterdam, The Netherlands: OMAE2011-49118.

Xu, Q., Kim, J., Bhaumik, T., O'Sullivan, J., Ermon, J. 2012. Validation of HSV semisubmersible VIM performance by model test and CFD. In: Proceedings of the 31st International Conference on Ocean, Offshore and Arctic Engineering. Rio de Janeiro, Brazil: OMAE2012-83207.